Microtearing simulations in support of NSTX measurements

Walter Guttenfelder[1], S.M. Kaye[1], F.M. Poli[1], Y. Ren[1], J. Candy[2], R.E. Bell[1], B.P. LeBlanc[1], G.W. Hammett[1], D.R. Mikkelsen[1], H. Yuh[3], W.M. Nevins[4], E. Wang[4]

[1]PPPL, USA
[2]General Atomics, USA
[3]Nova Photonics Inc., USA
[4]LLNL, USA

College W&M
Colorado Sch Mines
Columbia U
CompX
General Atomics
INEL
Johns Hopkins U
LANL
LLNL
Lodestar
MIT
Nova Photonics
New York U
Old Dominion U
ORNL
PPPL
PSI
Princeton U
Purdue U
SNL
Think Tank, Inc.
UC Davis
UC Irvine
UCLA
UCSD
U Colorado
U Illinois
U Maryland
U Rochester
U Washington
U Wisconsin

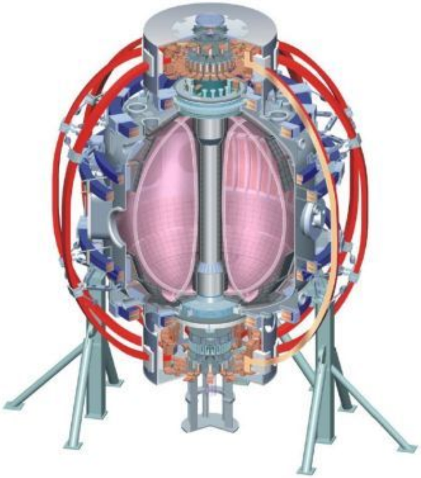

Culham Sci Ctr
U St. Andrews
York U
Chubu U
Fukui U
Hiroshima U
Hyogo U
Kyoto U
Kyushu U
Kyushu Tokai U
NIFS
Niigata U
U Tokyo
JAEA
Hebrew U
Ioffe Inst
RRC Kurchatov Inst
TRINITI
KBSI
KAIST
POSTECH
ASIPP
ENEA, Frascati
CEA, Cadarache
IPP, Jülich
IPP, Garching
ASCR, Czech Rep
U Quebec

Analyzing experimental discharges using gyrokinetic simulations (with GYRO*)

- Motivated by confinement scaling ($B\tau_E \sim \nu_*^{-0.95}$) in 2006 NSTX discharges (Kaye et al. 2007 PRL, NF)
  - Physical origin unclear, could influence design of next-generation device at low ν_*

- Microtearing unstable in high ν_* discharge (120968, 0.7 MA, 0.35 T, 4 MW, no Li)
  - Scaling of linear growth rates $\gamma_{lin} \sim \nu_e$, consistent with XP trend

⇒ **First <u>non-linear</u> microtearing simulations in NSTX**

  - Significant transport predicted, sensitive to E×B shear
  - Narrow density perturbations ($k_r > k_\theta$), potentially "observable" with high-k scattering

- Beginning to apply synthetic diagnostic to both microtearing and ETG simulations for comparison with high-k measurements (see APS posters by F.M. Poli & Y. Ren)

---

*J. Candy & R.E. Waltz, Phys. Rev. Lett **91**, 045001 (2003); J. Comp. Physics **186**, 545 (2003); https://fusion.gat.com/theory/Gyro

Linear microtearing instability

- High-m tearing mode around a rational $q(r_0)=m/n$ surface ($k_{||}(r_0)=0$)
  (Classical tearing mode stable for large m, $\Delta'\approx-2m/r<0$)
- Driven by ∇T_e with* (i) parallel thermal force or (ii) trapped-passing boundary effects $\Rightarrow$ *requires collisionality*

Conceptual linear picture

- Imagine helically resonant (q=m/n) δB_r perturbation $\delta B_r \sim \cos(m\theta - n\varphi)$
- δB_r leads to radially perturbed field line, finite island width $w = 4\left(\frac{\delta B_r}{B}\frac{rR}{n\hat{s}}\right)^{1/2}$
- ∇T_e projected onto field line gives parallel gradient $\nabla_{||}T_{e0} = \frac{\vec{B}\cdot\nabla T_{e0}}{B} = \frac{\delta B_r}{B}\nabla T_{e0}$
- Parallel thermal force ($R_{T||}\approx-n_e\nabla_{||}T_e$) drives parallel electron current that reinforces δB_r → instability
- Requires sufficient ∇T_e, β, ν_e, and positive magnetic shear (dq/dr)

*e.g. Drake & Lee, Phys. Fluids **20**, 1341 (1977); Catto & Rosenbluth, Phys. Fluids **24**, 1655 (1981); Connor, Cowley & Hastie, PPCF **32**, 799 (1990)

Microtearing modes unstable in high ν_* discharge 120968

- Microtearing dominates $k_\theta\rho_s<1$ in outer half-radius (r/a=0.5-0.8)
  - Resonant tearing parity in $A_{||}$ ($\delta B_r=-ik_\theta A_{||}$)
  - Extended potential eigenfunctions in ballooning space
  - Real frequencies in electron diamagnetic direction, $\omega \approx \omega_{*e} = (k_\theta\rho_s)\cdot(a/L_n+a/L_{Te})\cdot(c_s/a)$
- ETG becomes unstable at outermost locations (r/a=0.7-0.8, not shown)

real frequencies

ω_r (c_s/a)

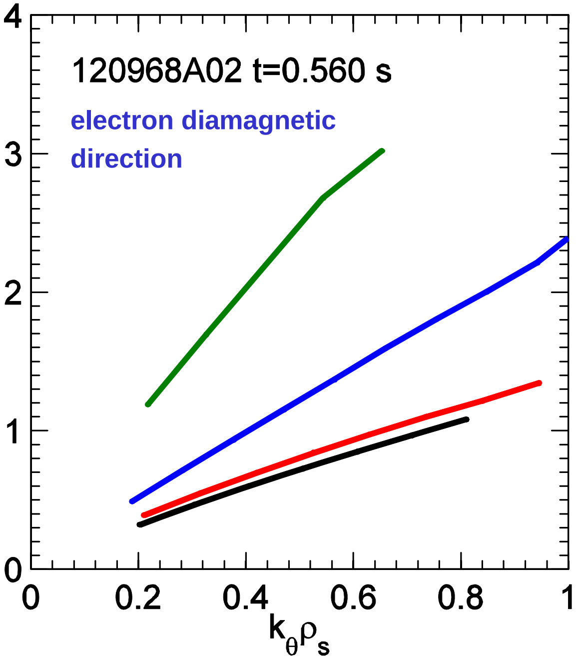

growth rates

γ (c_s/a)

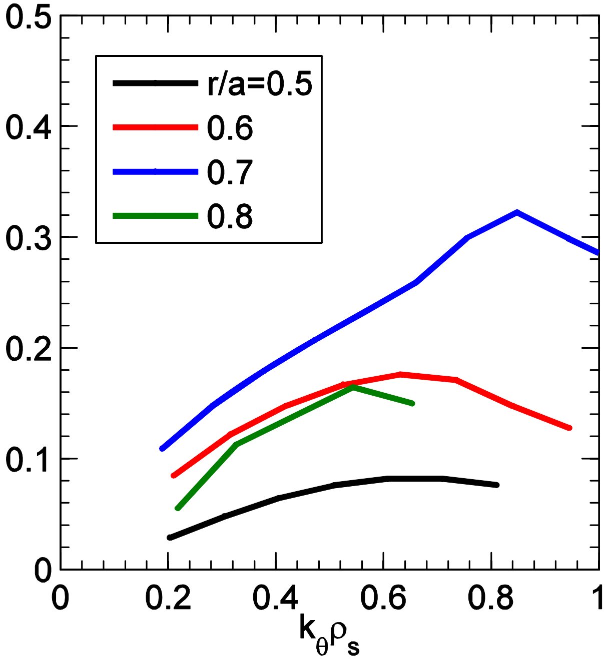

Eigenfunctions in “ballooning” space

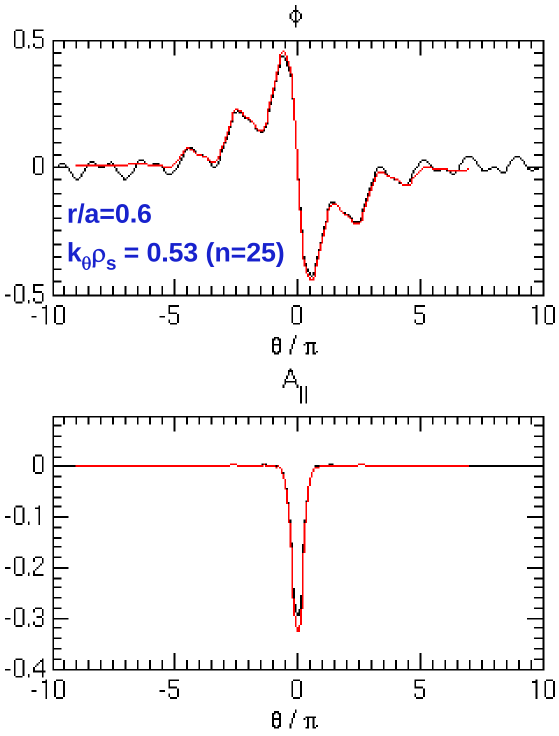

Microtearing instability exhibits thresholds in electron temperature gradient, collisionality and beta

(1) Apparent threshold in ∇T_e, $(a/L_{Te})_{crit} \approx 1.3\text{-}1.5$ $(a/L_{Te,exp}=2.7)$

(2) Growth rates decrease with $\nu_e < \nu_{e,exp}$ (consistent with experimental ν_* scan)

- Scaling with ν_e not simply monotonic – transition to TEM at very low ν_e

(3) Lowering beta stabilizes microtearing

- KBM becomes unstable at much larger β_e (not shown)

Linear growth rates ($\gamma \cdot a/c_s$) for NSTX 120968 t=0.56 s r/a=0.6

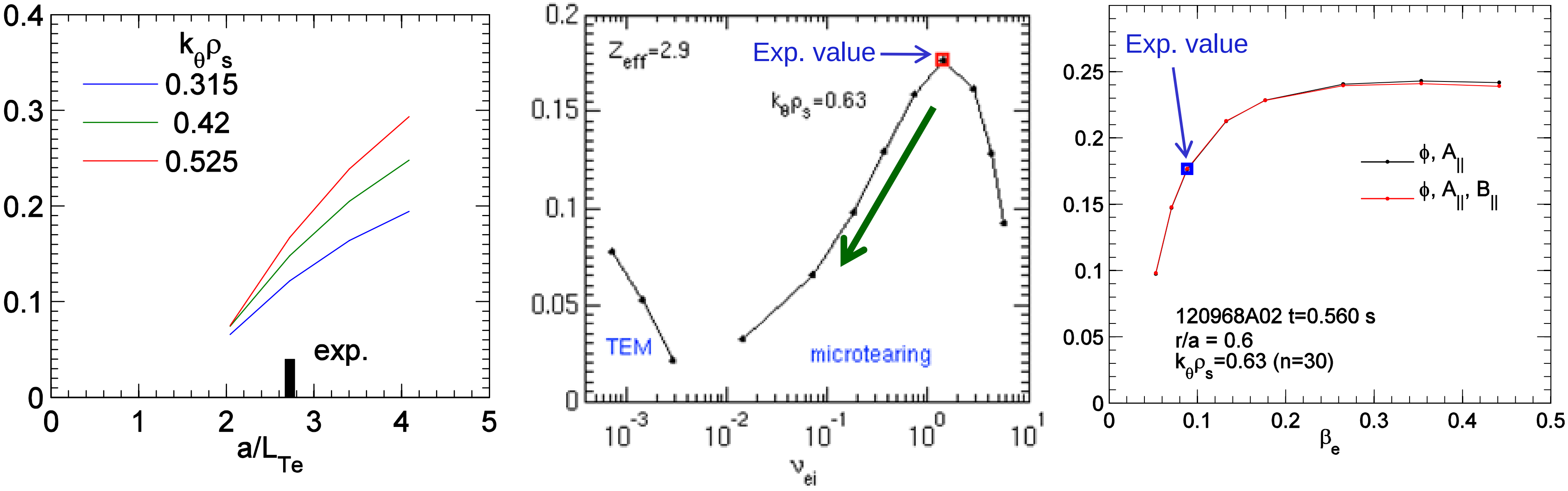
(1) (2) (3)

Nonlinear microtearing transport comparable to experimental transport

- With <u>no</u> E×B shear predicted transport (1.2 $\rho_s^2 c_s/a$) comparable to experimental transport (1.0-1.6 $\rho_s^2 c_s/a$)
- Transport reduced when increasing γ_E to local experimental value

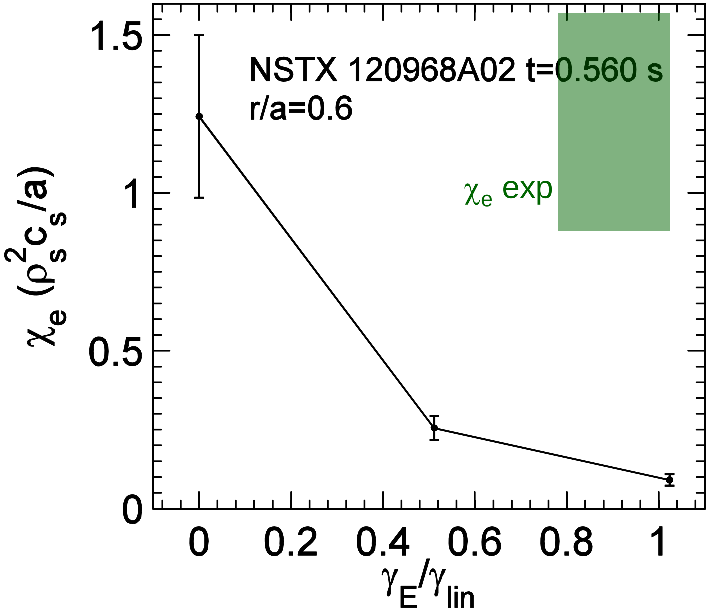

$\rho_s^2 c_s/a = 5\ m^2/s$

- Simulations are underway to investigate sensitivity to a/L_{Te}, β_e, ν_e

- Above are local simulations, but $\rho_s/a=0.08$ & physical domain r/a=0.3-0.9 → have not investigated influence of profile variations, e.g. $a/L_{Te}(r)$, $\gamma_E(r)$, q(r)

97% of transport in non-linear simulation due to electromagnetic contribution

- $w_{island}(n) > \Delta r_{rat}(n)$, island overlap → perturbed field line trajectories are stochastic
- $\chi_{e,EM}$ well described by *collisionless* Rechester-Rosenbluth (λ_{mfp}=25 m, L_c=2.5 m)*

→ APS invited talk by Eric Wang (submitted to Phys. Plasmas)

$$w_{island} = 4\sqrt{\frac{\delta B_{r,n}}{\underline{B}}\frac{rR}{n\hat{s}}} \qquad (\Delta r)_{rat} = \frac{1}{nq'} = \frac{1}{k_\theta \hat{s}}$$

from simulation

integrating dl/B
3000 transits for each
of 100 field lines

f_p≈50% passing particles

$$\chi_{st} \approx 2\left(\frac{2}{\pi}\right)^{1/2} D_{st} v_{te} f_p$$

$$D_{st} = \lim_{s\to\infty} \frac{\langle [r_i(s) - r_i(0)]^2 \rangle}{2s}$$

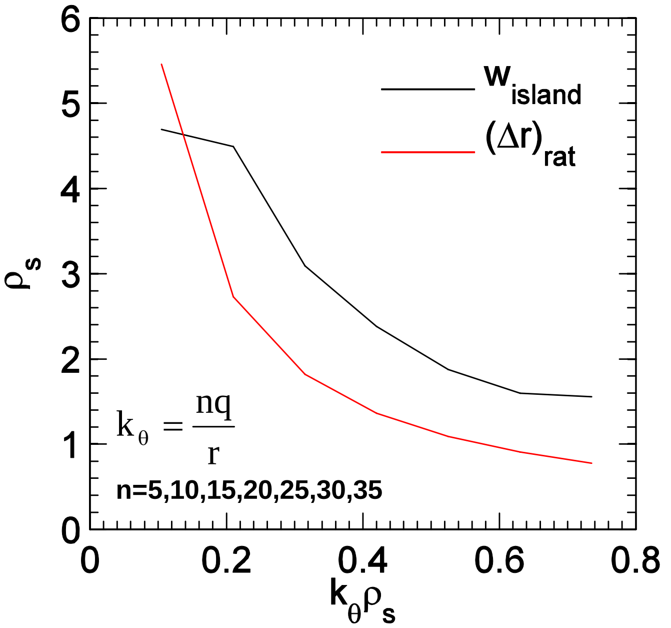

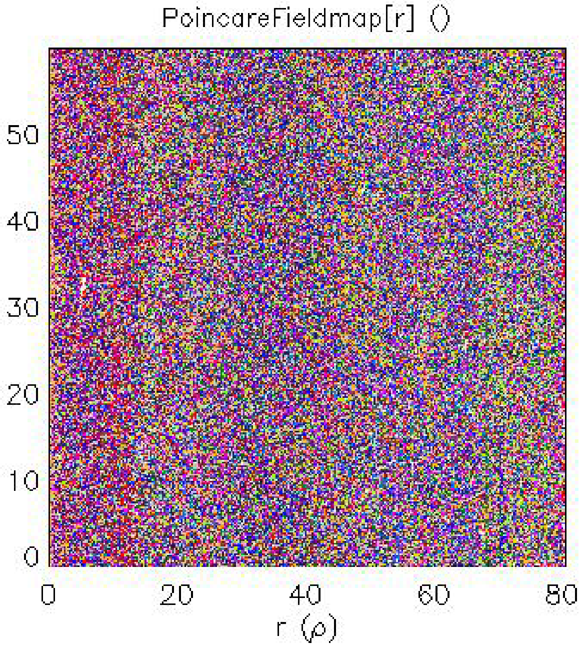

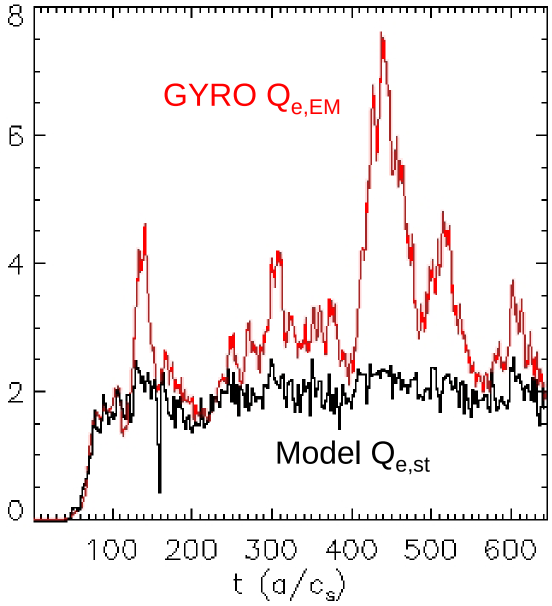

---

* A.B. Rechester & M.N. Rosenbluth, Phys. Rev. Lett. **40**, 38 (1978); R.W. Harvey et al., Phys. Rev. Lett. **47**, 102 (1981).

Nonlinear simulations exhibit narrow density & broad EM perturbations

- Narrow radial n, φ, $j_{||}$ structures need to be resolved but $A_{||}$ very broad = expensive
- $\delta B_r/B \sim 8.7\times10^{-4} \sim \rho_e/L_{Te} = 3.4\times10^{-4}$
  - $\delta B_r/B \sim \rho_e/L_{Te}$ analytic approximation from Drake et al. PRL 1980; used for NSTX in Wong et al. PRL 2007

$\delta n/n \approx 0.5\%$

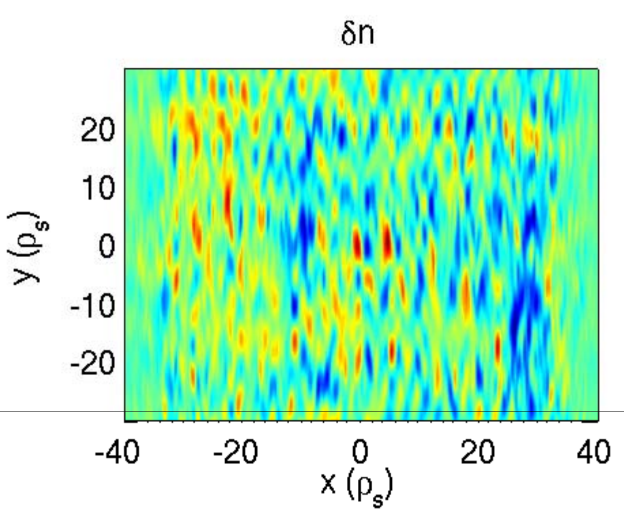

$\delta A_{||}/c_sT_e \approx 0.8\%$

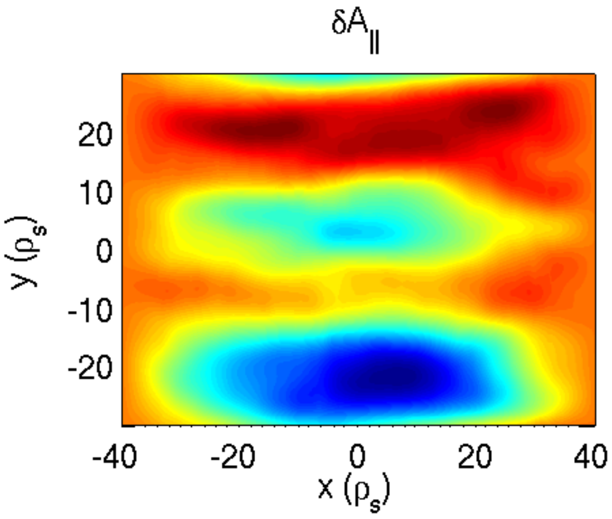

$\delta B_r/B \approx 0.09\%$

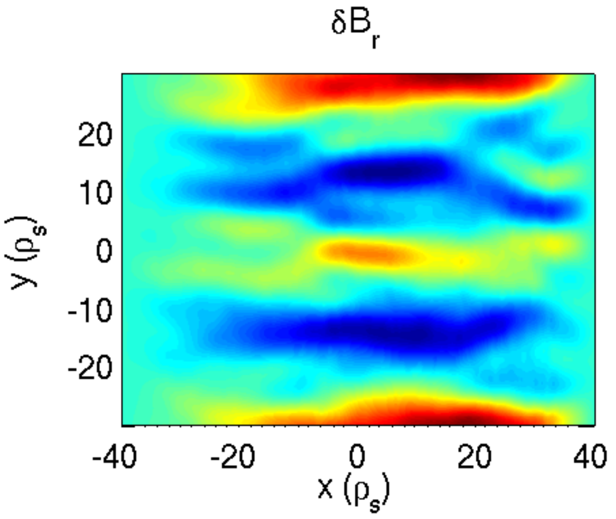

$\delta T_e/T_e \approx 2\%$

$\delta v_{e,||}/c_s \approx 6\%$

May expect significant intensity in high-k scattering from microtearing

- Comparable δn/n predicted for ETG (2.8×10^{-3}) and microtearing (1.7×10^{-3})
- But ETG spectrum much broader in $k_\theta\rho_s$ → less intensity per unit $\Delta k_x \cdot \Delta k_y$
- Application of synthetic "high-k" diagnostic beginning (see talks & APS posters by F.M. Poli & Y. Ren)

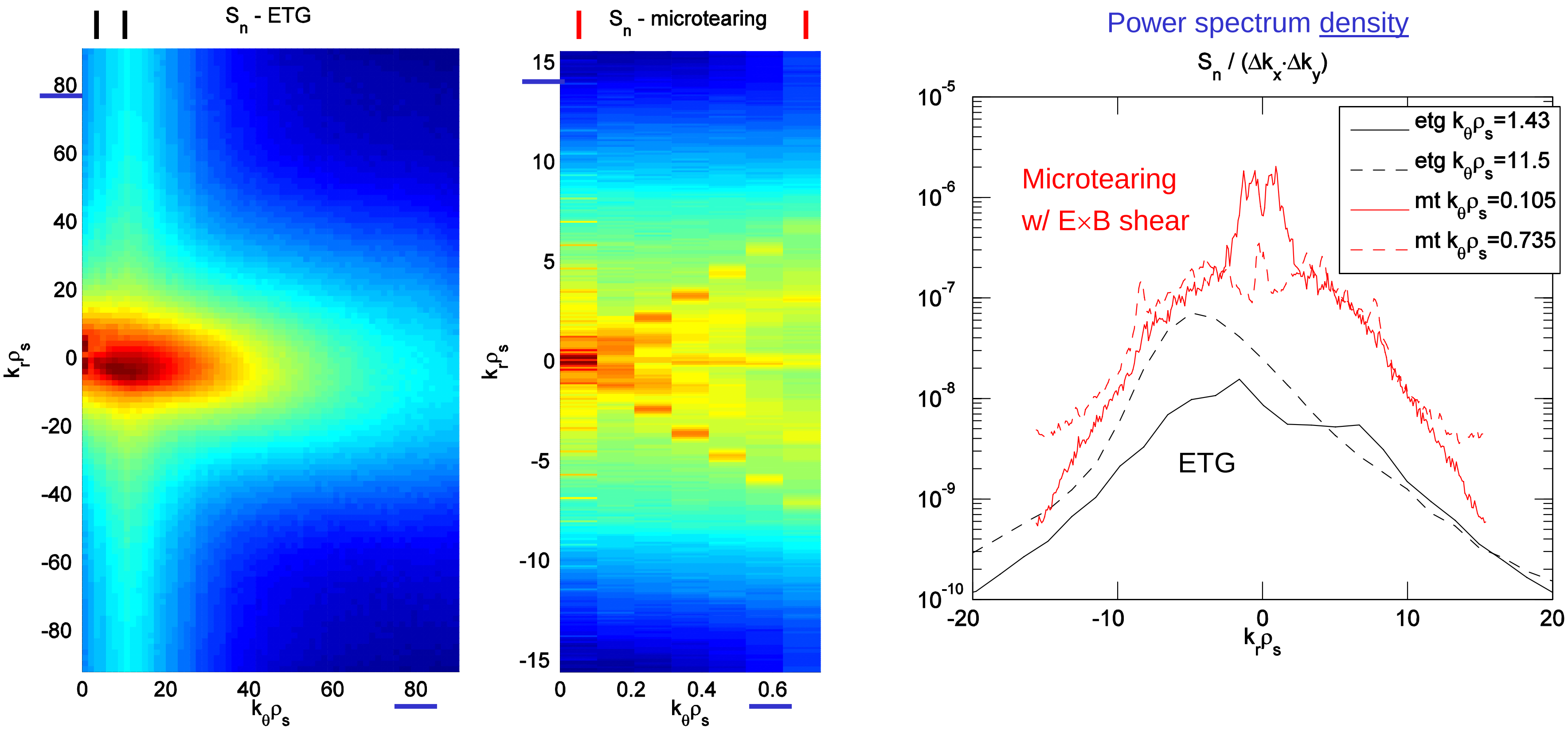

BACKUP SLIDES

Dimensionless ν^* scans – basis of microstability analysis

$$\begin{aligned} q &\sim I_p / B \\ \rho_* &\sim T^{1/2} / B \\ \beta &\sim nT / B^2 \end{aligned} \quad \Longrightarrow \quad \begin{aligned} I_p &\sim B \\ T &\sim B^2 \\ n &\sim B^0 \end{aligned} \qquad \boxed{\nu_* \sim B^{-4}}$$

NSTX 120968 I_p / B_T / P_{NBI} - 0.7 MA / 0.35 T / 4 MW

NSTX 120982 I_p / B_T / P_{NBI} - 1.1 MA / 0.55 T / 4 MW

Strong rotation and rotation shear

Ion transport well described by neoclassical (NCLASS)

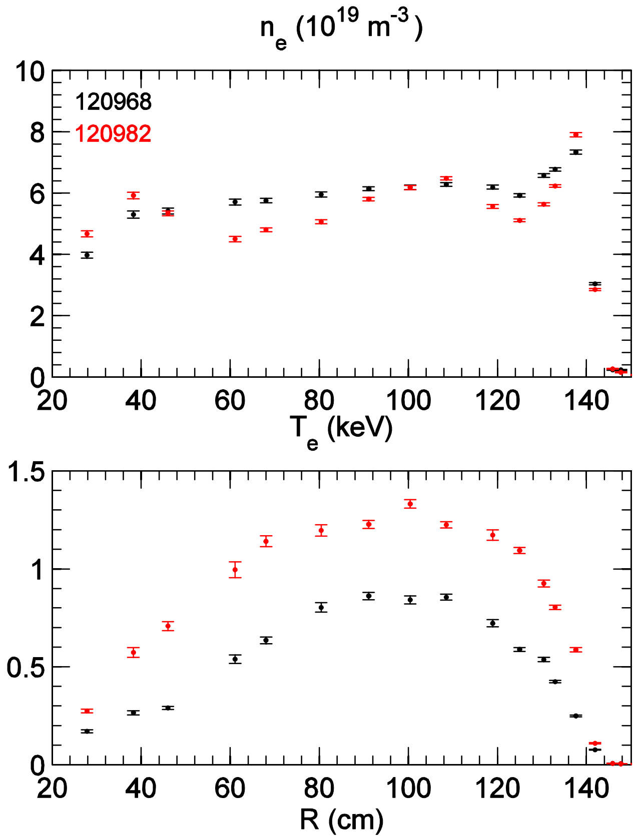

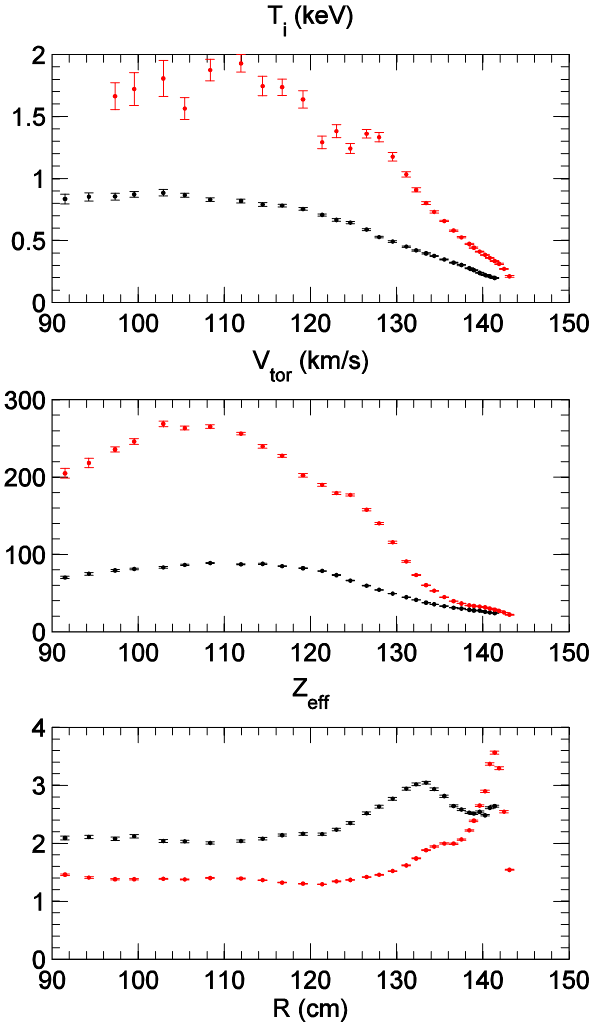

Experimental profiles of dimensionless parameters

Factor ~5 variation in ν_*, additional (non-ideal) variation in other dimensionless parameters

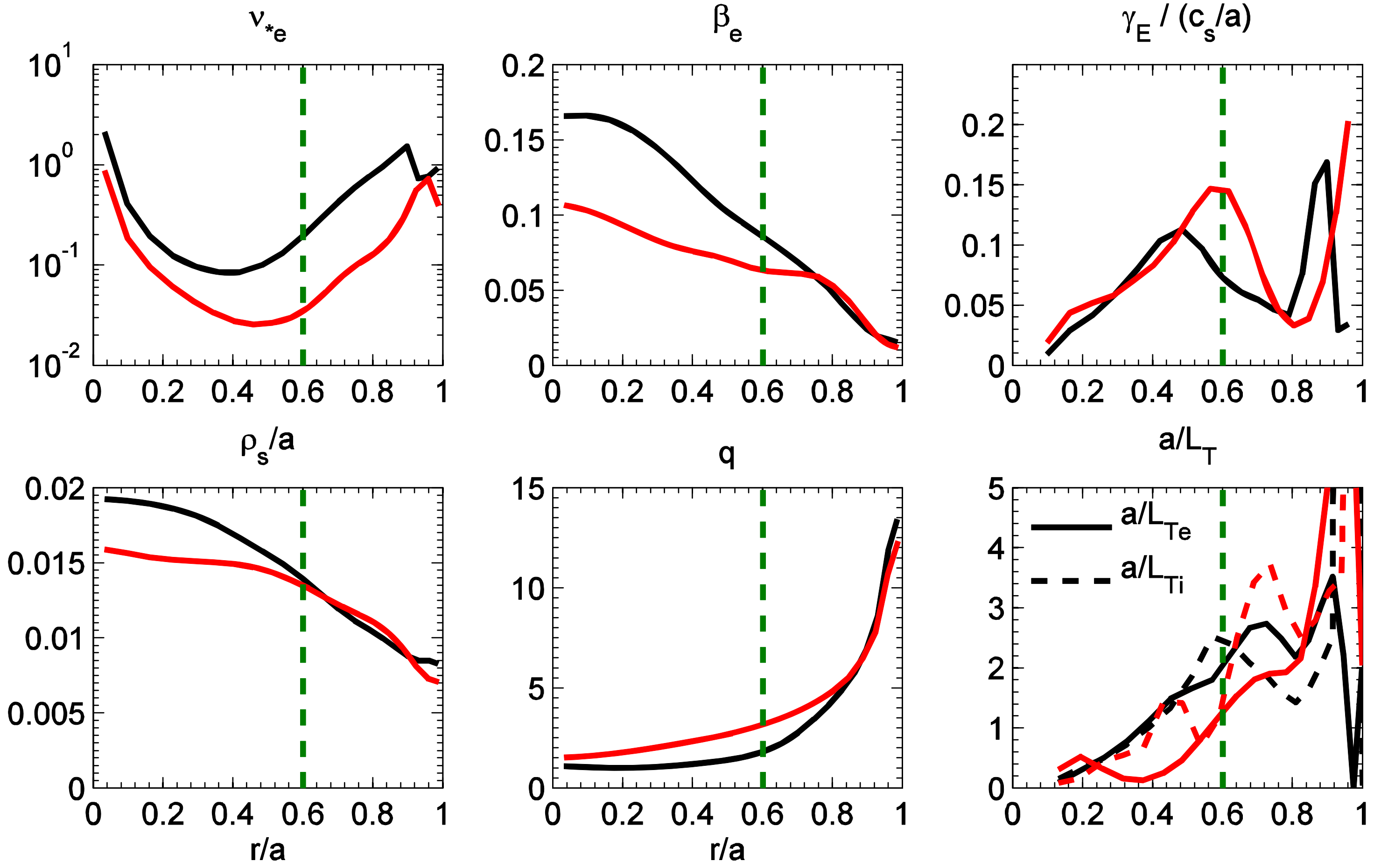

The following simulations are based on high ν_* NSTX discharge 120968 (mostly r/a=0.6)

Calculations were also performed for MAST discharges with similar results (not shown)

Linear mode structure in perpendicular (r,α) plane illustrates microtearing mode dynamics

- Narrow resonant current channel ($\approx 0.3\rho_s$) centered on rational surface
- "Constant ψ" ($A_{||}$), resonant tearing parity
- Nearly unmagnetized/adiabatic ion response $\Rightarrow \frac{\tilde{n}}{n_0} \approx -\left(\frac{e\tilde{\varphi}}{T_i}\right)$
- Narrow potential, density, T_e perturbations

field line label
$\alpha=\varphi-q\theta$ for low β
circular surfaces

"ballooning" space

$$k_r(\theta)=\hat{s}k_\theta(\theta-\theta_0)$$

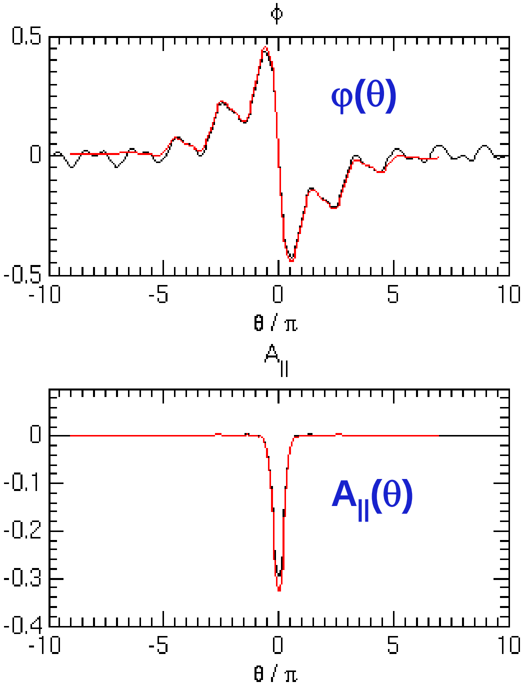

r-α perpendicular plane (θ=0)

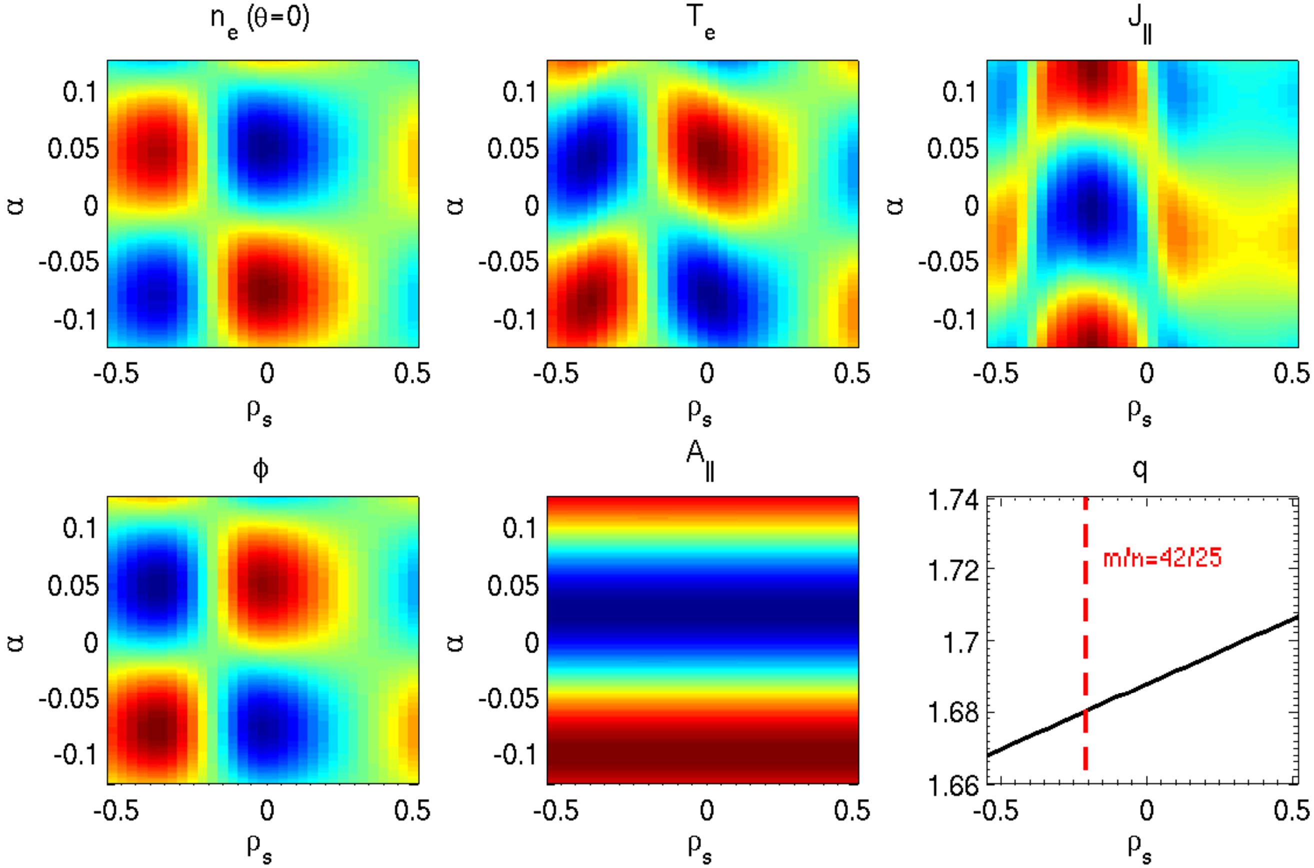

Linear mode structure in toroidal (R,Z) plane

- Nonuniform poloidal structure (comparing inboard and outboard perturbations)
- Density perturbations radially narrow, extended vertically on outboard side

⇒ “High-k” scattering diagnostic well suited for $k_r >> k_\theta$

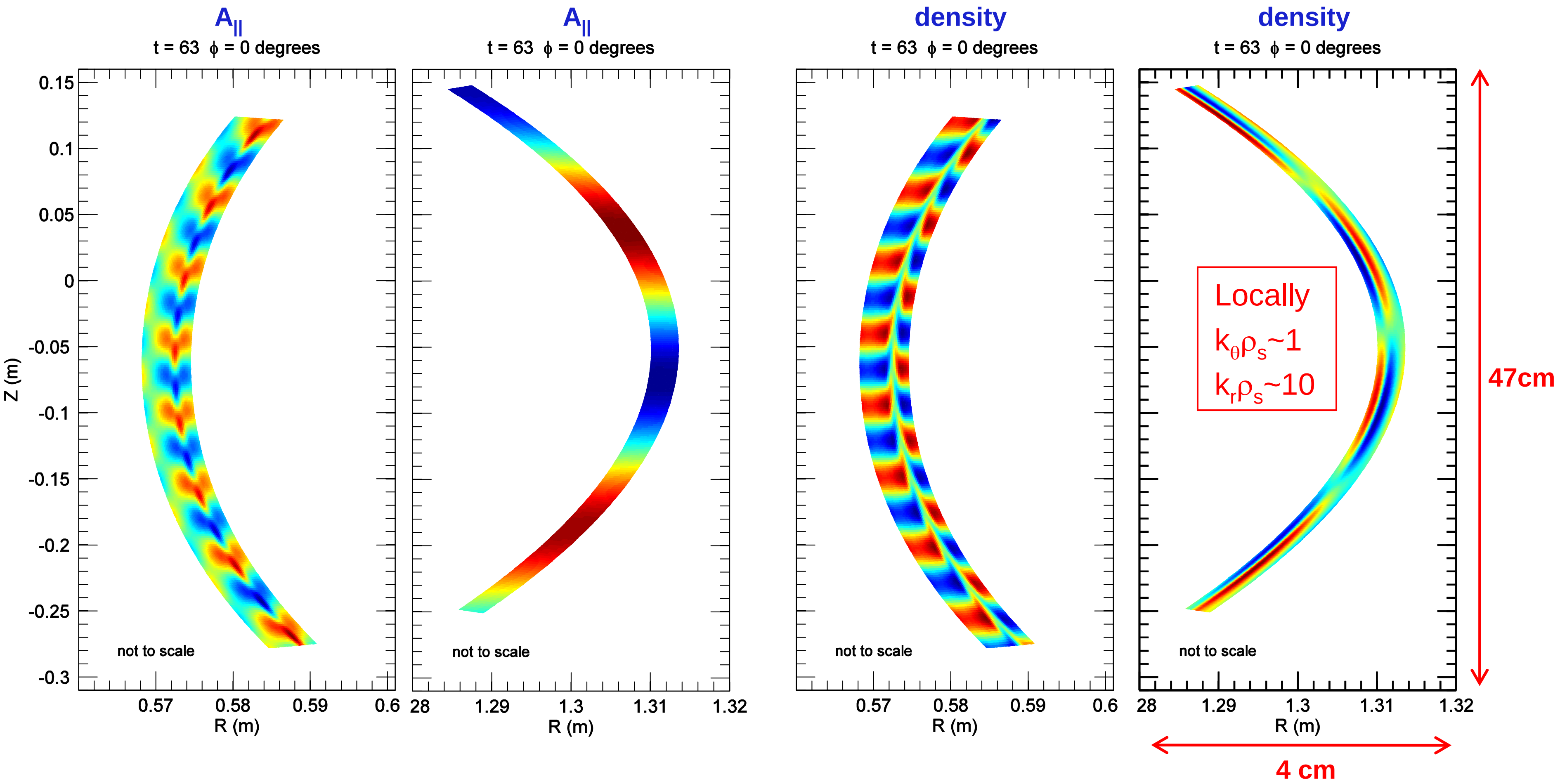

Locally
$k_\theta \rho_s$~1
$k_r \rho_s$~10

47cm

4 cm

Field line integration used to map island

- δB_r in linear run (arbitrary) determines $w_{island} \sim 0.4\ \rho_s$
- Slab/cylindrical island width estimate does not work well (δB_r strongly ballooning)

$$\left|\frac{\delta B_{r,mn}}{B}\right| = 1.8 \cdot 10^{-7}$$

$$w = 4 \cdot \left[\frac{\delta B_{r,mn}}{B}\frac{rR}{n\hat{s}}\right]^{1/2} \underline{= 0.03\rho_s}$$

- Estimate using rms δB_r gets closer

$$\left|\left\langle\frac{\delta B_r^2}{B^2}\right\rangle_{\alpha,\theta}\right|^{1/2} = 2.5 \cdot 10^{-5}$$

$$w = 4 \cdot \left[\left(\frac{\delta B_r}{B}\right)_{rms}\frac{rR}{n\hat{s}}\right]^{1/2} \underline{= 0.39\rho_s}$$

- $w_{island}/L_{Te} \approx 8 \cdot 10^{-3}$ but $\max(\delta T_e/T_e) \approx 4.5 \cdot 10^{-4}$

⇒ Influence of perpendicular drift dynamics

Poincare plot & contours of parallel current

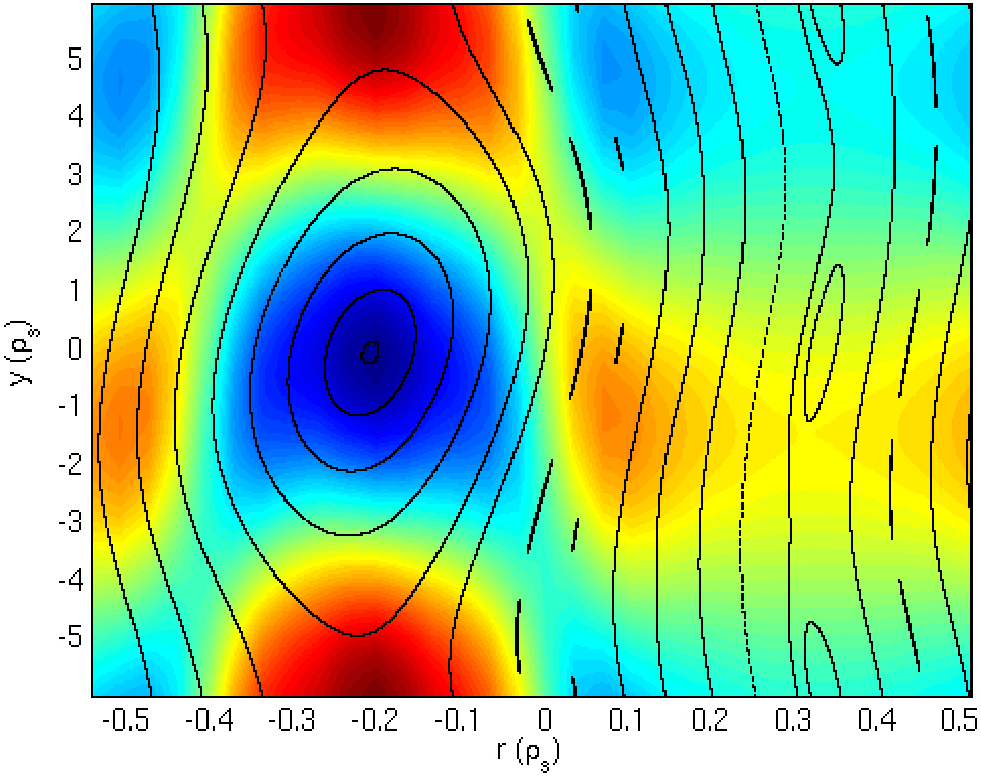

Fine radial resolution required to capture *linear* resonant layers

Calculating linear growth rate for single mode ($k_\theta \rho_s$=0.63, n=30) using box width and resolution of nonlinear simulations

L_x=80 ρ_s, Δx=0.4 & 0.2 ρ_s

(1) Δx=0.4 ρ_s is barely small enough to distinguish resonant layers

(2) Δx=0.2 ρ_s resembles the...

(3) high resolution flux-tube case

(1)
L_x = 80 ρ_s
nx = 200

(2)
L_x = 80 ρ_s
nx = 400

(3)
"Typical" flux tube
L_x = 0.9 ρ_s = $(\Delta r)_{rat}$
nx = 32

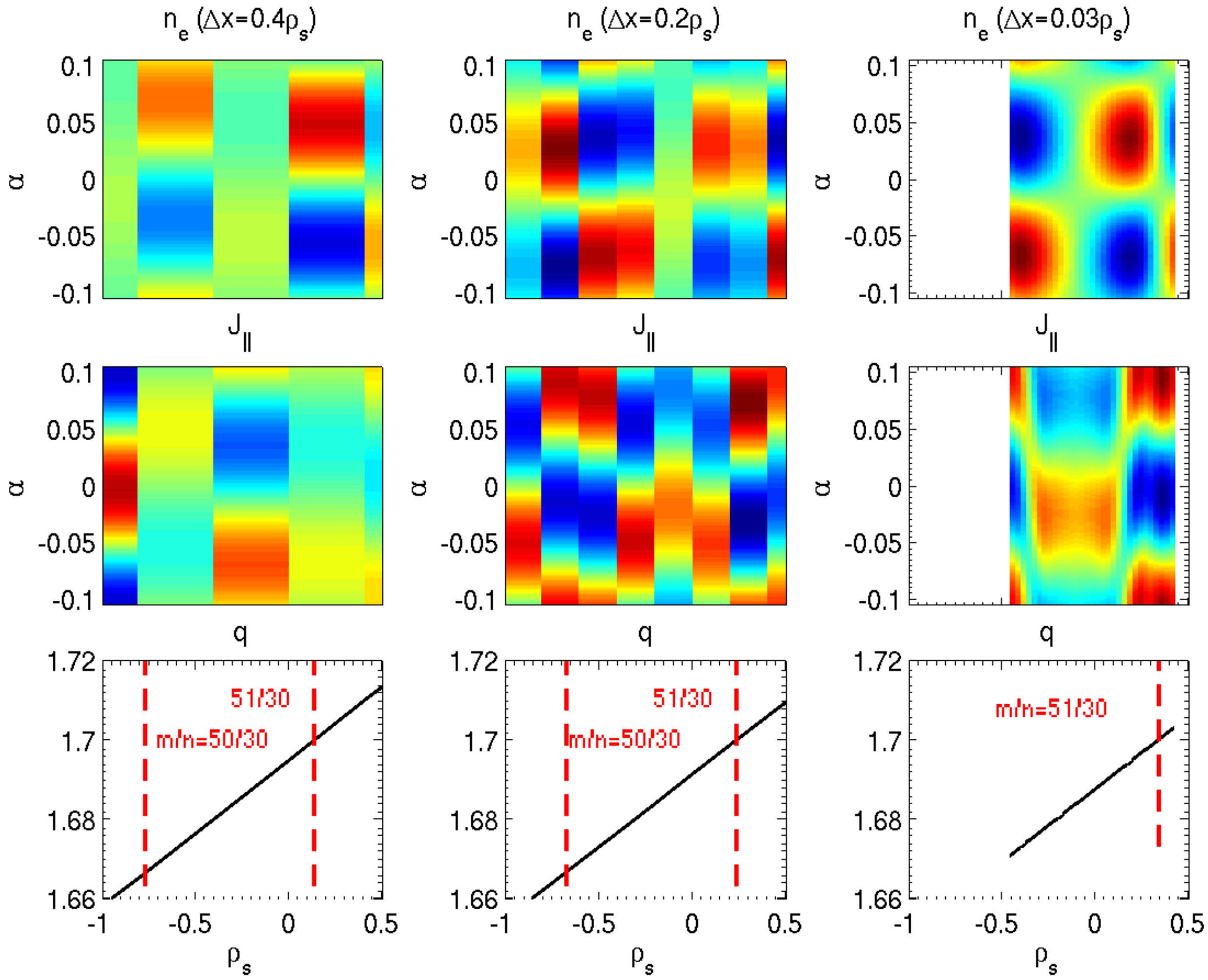

Fine radial resolution required for resolved *nonlinear* spectra

- k_x spectra completely different for $\Delta x = 0.4 \rightarrow 0.2 \rho_s$
- Insufficient resolution leads to peaking at high k_x similar to GS2 simulations in Applegate Ph.D. thesis (2007, Imperial College London)

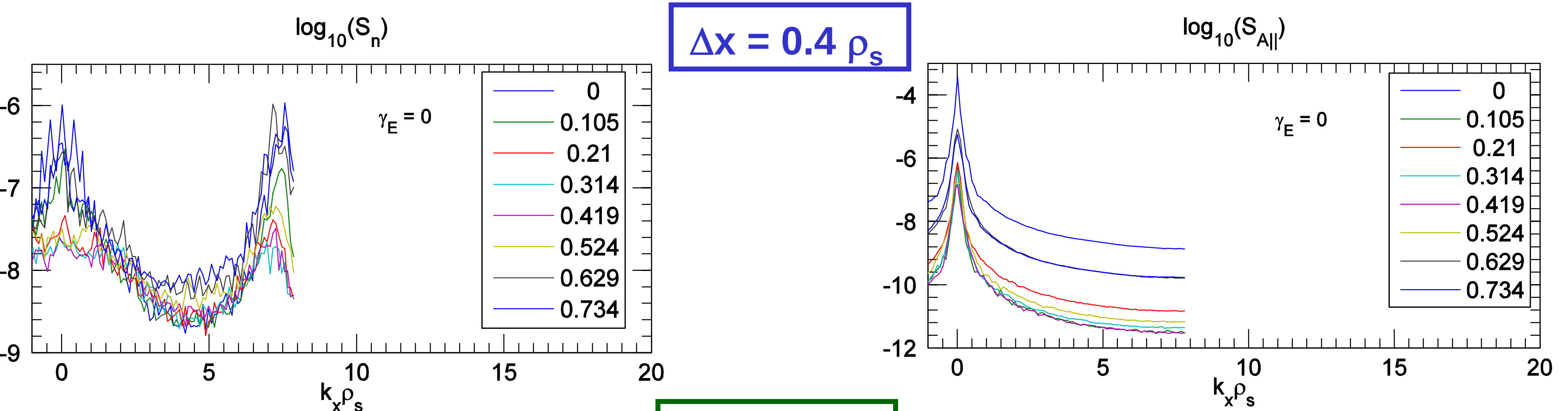

$\Delta x = 0.4\ \rho_s$

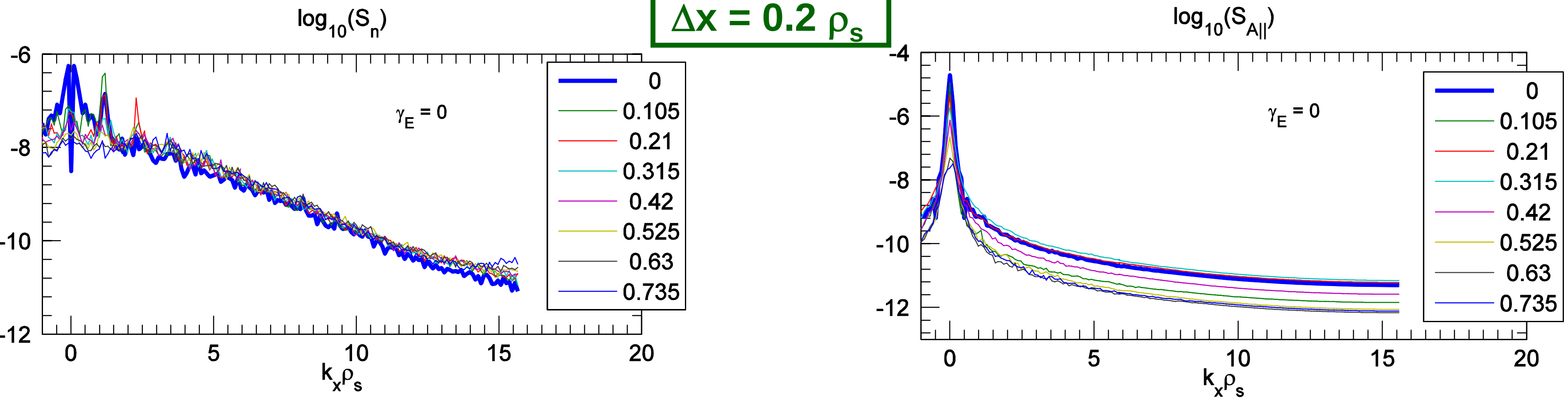

$\Delta x = 0.2\ \rho_s$